Topography and Surface Composition of Thin Films of Blends of Poly(methyl methacrylate) and Poly(ethylene oxide)

Stanley Affrossman,*,† Thomas Kiff,‡ Scott A. O'Neill,† Richard A. Pethrick,† and Randal W. Richards‡

Department of Pure and Applied Chemistry, University of Strathclyde, Thomas Graham Building, Cathedral Street, Glasgow G1 1XL, UK, and Interdisciplinary Research Centre in Polymer Science and Technology, University of Durham, Durham DH1 3LE, England

Received May 20, 1998; Revised Manuscript Received September 3, 1998

ABSTRACT: Thin films of PMMA−PEO blends have been formed by spin casting. The AFM images of PEO-rich films have an angular character associated with the crystallinity of the polyether. Addition of PMMA produces more rounded submicron features with height of the order of nanometers, which annealing studies suggest are PMMA-rich regions. Heating for an hour above the T_g of PMMA leaves a smooth surface. The topographical features are postulated to arise from metastable phases formed during the solvent evaporation. For a series of blends of constant composition with varying molecular weights of PMMA, a linear relationship is obtained for the average height of the features versus the radius of gyration of PMMA, with the step height corresponding to four PMMA molecules. The surface compositions of the films were determined by XPS and SIMS. Segregation of PMMA, observed for unannealed, low PMMA content blends, is ascribed to the partial crystallinity of the films, while higher PMMA content blends have similar surface and bulk compositions.

Introduction

Several studies have been made of blends of poly(ethylene oxide), PEO, and poly(methyl methacrylate), PMMA, encompassing mixtures of components of various molecular weights, and the system is accepted to be compatible in the melt in accordance with the calculated χ values.[1−4] Nevertheless, phase segregation is frequently observed in solid PEO−PMMA blends because of the crystalline nature of PEO, which gives rise to a complex phase structure containing crystalline PEO and amorphous PEO−PMMA, the latter being incorporated between the PEO crystallites, plus an interface region consisting of PEO which is amorphous but excludes PMMA.[5] For a mixture of PMMA, M_w = 117K, and PEO, M_w = 20K, the amorphous PMMA phase is reported to have a composition ca. 90% w/w PMMA over a range of blend compositions.[4] Similarly, the amorphous phase in blends of PMMA, M_w = 90K, and PEO, M_w = 200K, has an approximately constant composition ca. 75% w/w PMMA for blends of PEO ≥ 30% w/w.[6] Generally, it is considered that blend compositions >70% w/w PMMA are almost completely amorphous, and NMR studies have shown that the homogeneity persists down to a level of the order of 2−70 nm.[6,7]

In addition to any complexities of bulk phase behavior, the structure of thin films of polymer blends is influenced by the substrate−polymer and polymer−air interfaces. Light transmission has been used to observe differences in phase separation behavior for PEO−PMMA films up to 60 μm in thickness cast on hydrophilic or hydrophobic surfaces.[8] Recent atomic force microscopy, AFM, studies have shown that the polymer−air surface of thin, cast films of blends of incompatible polymers may exhibit topography, with surface features of lateral dimension in the 0.1−1.0 μm range and height of the order of nanometers.[9−15] The formation of topographical features depends on the chemical nature of the substrate surface and the degree of incompatibility of the polymers,[13] which can be estimated from the interfacial width of bilayers of the blend components. Amorphous (high PMMA content), thin, cast films of PEO−PMMA blends may not be expected to exhibit submicron topographical features at the polymer−air interface in view of the compatibility of the components and the evidence of lack of heterogeneity in the bulk amorphous phase down to nanometer dimensions.[6,7] On the other hand, the formation of crystalline PEO phases in lower PMMA content blends would induce heterogeneity into the system, and traces of crystalline PEO have been noted even in blends with 80% w/w PMMA.[4] Further, it has been shown that on cooling the melt a phase separation can occur before crystallization.[4] With the rapid solvent evaporation during formation of a spun thin film, intermediate phase structures may become "frozen in" because of the sudden onset of restricted mobility of the polymer chains. Preliminary experiments showed marked topography with certain PEO−PMMA blends. Therefore, the physical structure and surface chemical composition of a series of PEO−PMMA thin films are investigated in this report to determine the origin and nature of the topography.

Experimental Section

Materials. Initial experiments to determine optimum casting conditions were carried out with high-polydispersity polymers. Thereafter, high-purity, low-polydispersity materials produced by anionic polymerization were used. Table 1 lists the origins and characteristics of the polymers.

Film Formation. The blend components were dissolved in chloroform at a total concentration of 1% w/w, unless otherwise stated.

The details of film formation, AFM operation, and the conditions for X-ray photoelectron spectroscopy, XPS, and

† University of Strathclyde.
‡ University of Durham.
* To whom correspondence should be addressed.

10.1021/ma980804n CCC: $18.00
Published on Web 03/19/1999

Table 1. Polymer Characteristics

polymer	M_n, kg mol^{-1}	M_w/M_n	supplier
PEO1	28	7.0	Aldrich
PEO2	11	1.10	Polymer Lab
PEO3	116	1.07	Polymer Lab
PEO4	118	1.02	synthesized
PMMA1	37	2.6	Aldrich
PMMA2	54	1.2	Polymer Lab
PMMA3	71	1.1	Polymer Lab
PMMA4	114	1.29	synthesized
PMMA5	138	1.04	Polymer Lab
PMMA6	320	1.3	Polymer Lab

secondary ion mass spectroscopy, SIMS, analysis are given in a previous publication.[9] Films were cast by dropwise addition of the blend solution to the substrate spinning at 4000 rpm. AFM images were obtained with the Burleigh 5 μm × 5 μm head. Average feature heights were obtained from line profiles using the statistical package provided. Several line profiles were measured, and a mean value was taken. Film thickness was determined with a Sloan Dektak 11a profilometer.

XPS/SIMS. In PEO all the carbons in the polymer are chemically equivalent. Therefore, the XPS C 1s signal from PEO consists of a single peak corresponding to carbon joined to a single oxygen atom, and the C 1s chemical shift, compared to carbon joined only to carbon, will be ca. 1.5 eV.[16] PMMA has a more complex C 1s envelope because there are four carbon environments,

$$-[C^aH_2.C^b.(C^aH_3).C^c(=O).OC^dH_3]-$$

The XPS instrument used was not monochromated, and the carbon C^b β-shift is only 0.4 eV.[16] Therefore, C^a and C^b were not distinguished, and only three carbon peaks, $C^{a/b}$, C^c, and C^d, were used to synthesize the C 1s envelope. Further, with mixtures of PMMA and PEO the binding energies of C^d and the PEO carbon are also similar, and the respective signals were evaluated as a single contribution, $C^{d/peo}$. Figure 1a/b shows the XPS C 1s envelopes for the PMMA homopolymer and a typical PMMA−PEO blend.

The method used to determine the component concentrations in the blend by XPS was to measure the distinct C^c peak and to utilize the known stoichiometry to separate the various contributions, i.e., noting that for PMMA the area of peak C^c = the area of peak C^d,

$$\text{total C 1s contribution of PMMA} = \text{peak } C^{a/b} + \text{peak } C^c + \text{peak } C^d$$

$$= \text{peak } C^{a/b} + 2(\text{peak } C^c)$$

$$\text{total C 1s contribution of PEO} = \text{peak } C^{d/peo} - \text{peak } C^d = \text{peak } C^{d/peo} - \text{peak } C^c$$

The concentration of PMMA monomer is $PMMA_{XPS} \propto$ [peak C^{ab} + 2(peak C^c)]/5, and the concentration of PEO monomer is $PEO_{XPS} \propto$ [peak $C^{d/peo}$ − peak C^c]/2. Therefore, the fraction PMMA monomer is $PMMA_{XPS}/[PMMA_{XPS} + 2.5PEO_{XPS}]$.

The SIMS spectra of the homopolymers were obtained, and the fragments at 69 and 45 Da were chosen as characteristic signals for PMMA and PEO, respectively. The relative intensities of the characteristic SIMS fragments were taken as measures of the component concentrations in the blend. The homopolymer spectra showed that both characteristic signals contained minor contributions from intrinsic peaks from the other polymer component and, possibly, impurities. These amounted to 0.04(PEO peak) for the PMMA peak and 0.15-(PMMA peak) for the PEO peak. In addition, the relationship between the characteristic peak intensities and the polymer concentrations was not known. It was not possible to synthesize a random copolymer of the components, which would have allowed direct determination of the relative SIMS sensitivity, S, where S is defined by

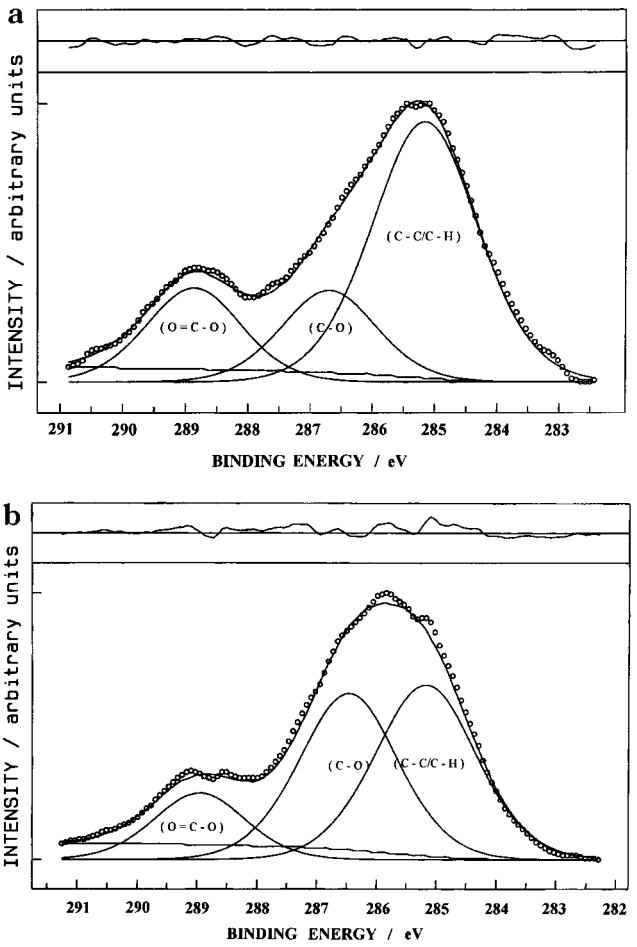

Figure 1. XPS C 1s envelope of (a) pure PMMA and (b) a typical PMMA−PEO blend.

$$\frac{\text{contribution to the 69 Da signal from PMMA}}{\text{contribution to the 45 Da signal from PEO}} = S \times \frac{\text{PMMA concentration}}{\text{PEO concentration}}$$

Thence, the total contributions to the 69 Da signal = S × (PMMA concentration) + 0.04 × (PEO concentration), and the total contribution to the 45 Da signal = (PEO concentration) + 0.15 × S × (PMMA concentration).

However, XPS measurements, discussed later, showed that the 75% w/w PMMA (0.57 PMMA monomer fraction) blend had similar surface and bulk concentrations. Accordingly, it was assumed that there was no concentration gradient in the surface region for this blend, which was chosen to calibrate the relative SIMS sensitivities from

$$\frac{I^{69}}{I^{69} + I^{45}} = \{S(\text{PMMA conc}) + 0.04(\text{PEO conc})\}/\{[S(\text{PMMA conc}) + 0.04(\text{PEO conc})] + [(\text{PEO conc}) + 0.15S(\text{PMMA conc})]\}$$

and gave a value for S of 0.6.

Various values of PMMA and PEO concentrations were substituted into the above equation to calculate the corresponding ratio of intensities, $I^{69}/(I^{69} + I^{45})$, which were then compared with measured intensity ratios to give the surface monomer fraction.

Results and Discussion

Effect of Film Thickness on Topography. Preliminary experiments on the effect of film thickness

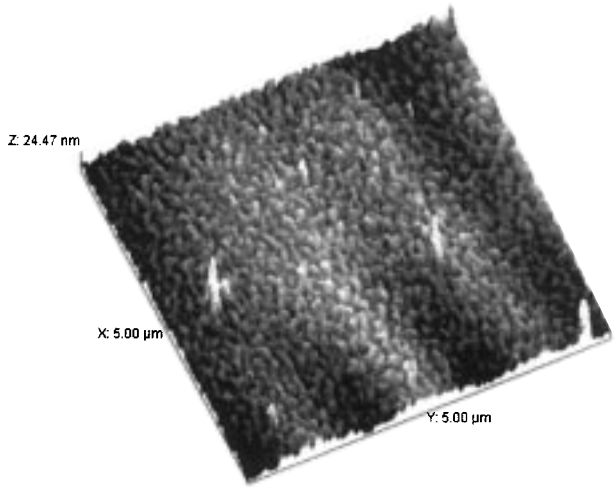

a 75%w/w PMMA 0.2% concentration.

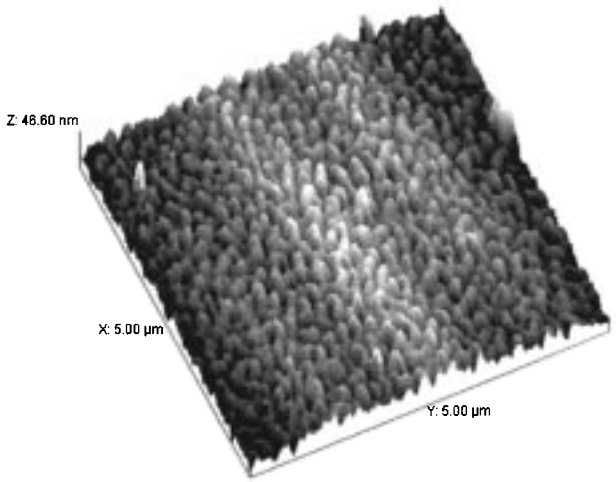

b 75%w/w PMMA 0.5% concentration.

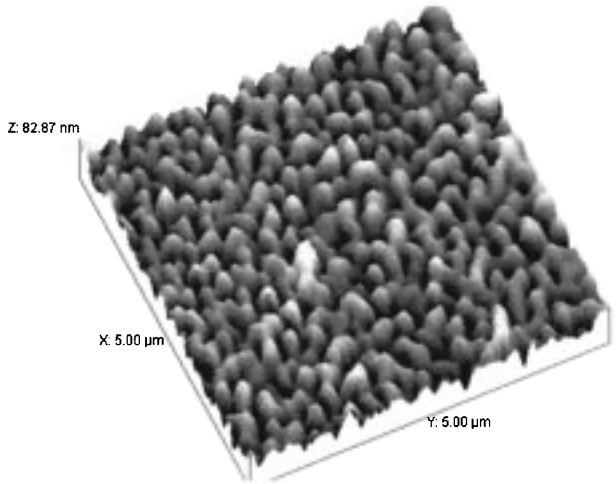

c 75%w/w PMMA 0.8% concentration.

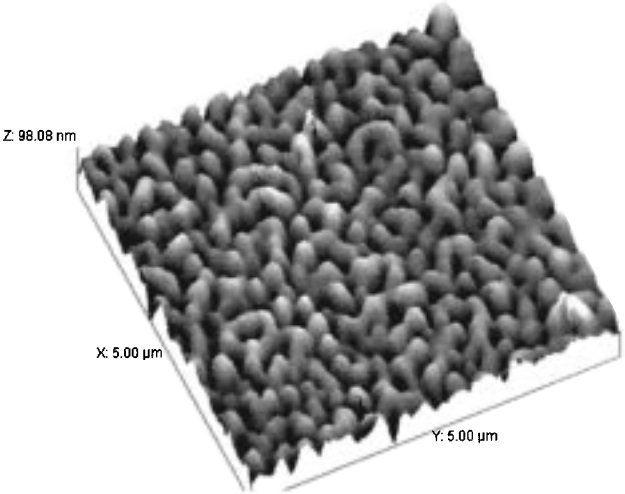

d 75%w/w PMMA 1.0% concentration.

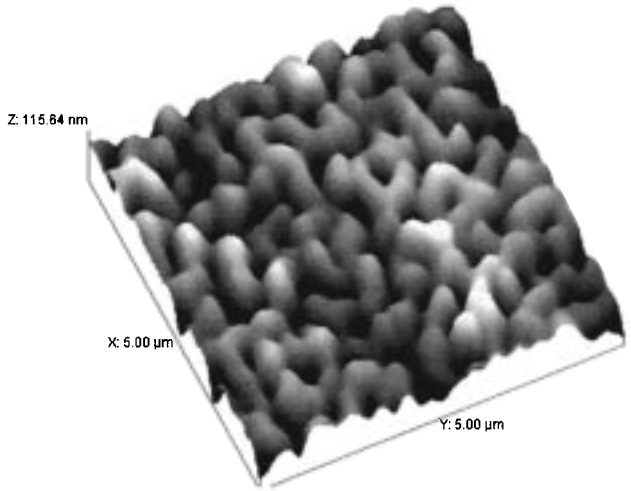

e 75%w/w PMMA 2% concentration.

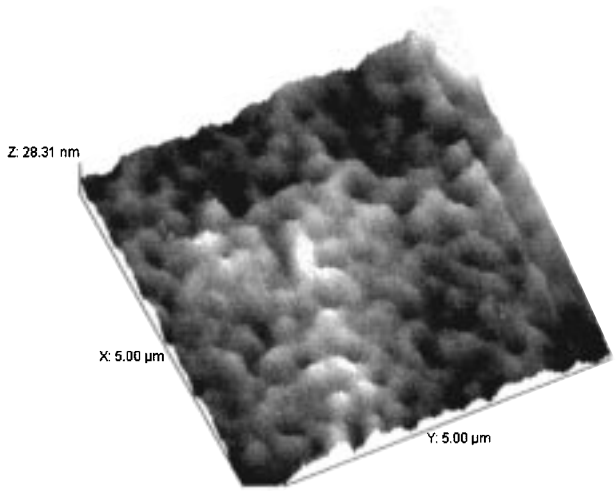

f 75%w/w PMMA 5% concentration.

were carried out with blends of PEO1 and PMMA1. The variations in film thickness were obtained by keeping the casting conditions and blend composition constant and varying the total polymer concentration. Figure 2 shows the AFM images for various film thicknesses of a 75% w/w PMMA blend, and Table 2 gives the film thickness and typical depth of topographical features. The film thickness increases monotonically with solution concentration. Even a film that was too thin to be measured accurately had marked features. The topographical features grow larger and more prominent, and the density per unit area becomes smaller as the thickness is increased. In the 100−200 nm thickness region the average depth of the features is 58 ± 8% of the film thickness, but by a thickness of 500 nm the depth decreases to 13%. For thicknesses of ≥ca. 500 nm

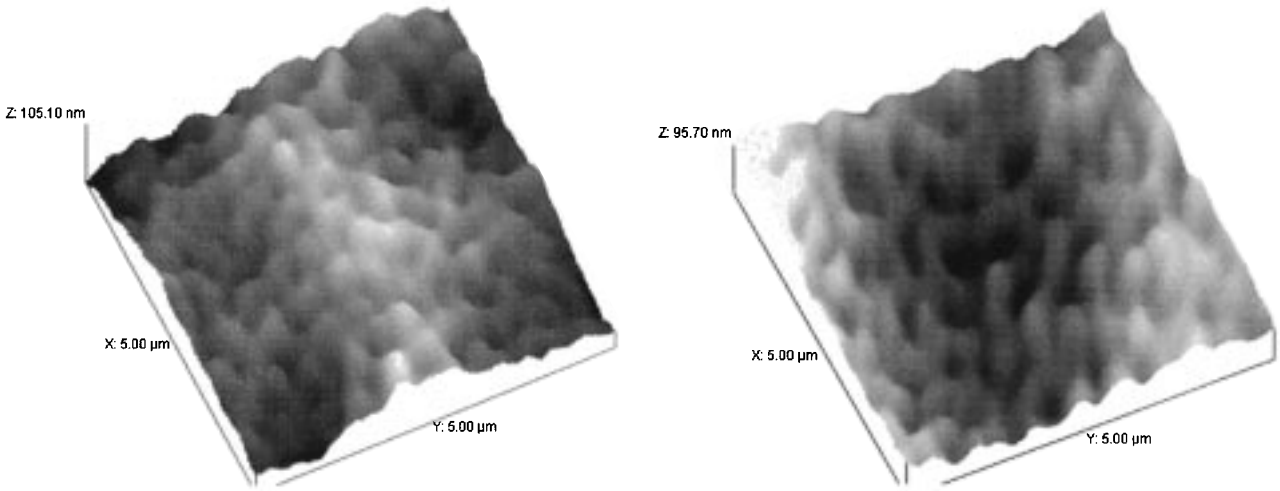

g 75%w/w PMMA 8% concentration. **h 75%w/w PMMA 10% concentration.**

Figure 2. Topography of a blend of 75% w/w PMMA1:25% w/w PEO1 cast from solutions of various concentrations. AFM images are 5 μm × 5 μm.

Table 2. Effect of Casting Solution Concentration on Film Thickness and Topography: Blend 75% w/w PMMA1:25% w/w PEO1

Figure	solution concn, % w/w	film thickness, nm	typical height/depth, nm
2a	0.2	*a*	11 ± 4
2b	0.5	50 ± 7	25 ± 4
2c	0.8	102 ± 10	66 ± 7
2d	1.0	182 ± 24	93 ± 18
2e	2.0	500 ± 95	64 ± 19
2f	5.0	5800 ± 4500	26 ± 5
2g	8.0	10700 ± 4400	54 ± 6
2h	10.0	*b*	60 ± 20

[a] Too thin to measure. [b] Too thick to measure.

the lateral dimensions of the features remain similar, but the depth decreases. The films chosen for the main part of this study had thicknesses <500 nm, but it must be noted that changes in topography as a consequence of variations in, say, blend composition also contain a factor from associated variations in film thickness.

Effect of Molecular Weight. A survey was made of the topography of several blends with components of various molecular weights. Blends were prepared at a constant composition of 75% w/w PMMA, and the cast films were examined by AFM (Figure 3a−e, Table 3). Keeping the PEO constant at 116K M_n, with PMMA of 54K and 71K M_n there was evidence of shallow topographical features. The ca. symmetric blend of 114K M_n PMMA and 116K M_n PEO gave pronounced features, as did a blend of 320K M_n PMMA and 116K M_n PEO. Making the blend more asymmetric, 114K M_n PMMA and 11K M_n PEO, resulted in a smooth film. The thickness of the films varied with the molecular weight and asymmetry of the blend components from 33 to 252 nm (Table 3). All these films would have been expected to have marked features on the sole criterion of film thickness. The reduced features of the asymmetric blends suggest a molecular weight effect; thus, the subsequent work was carried out with a ca. symmetric blend.

Topography and Film Thickness of Selected Homopolymers. The homopolymers PEO4 (M_n 118K, M_w/M_n 1.02) and PMMA5 (M_n 138K, M_w/M_n 1.04) were selected for more intensive study. AFM images of spun-cast films of the two homopolymers (Figure 4a/h) reflect the different characters of the materials. The surface of the amorphous PMMA is smooth, while the image of the semicrystalline PEO shows considerable roughness. Under the same casting conditions, the PEO film has a 3-fold greater overall thickness compared to that of PMMA (Table 4), which is attributed to the differences in film structure and, possibly, differences in solution viscosity, which is one of the factors controlling film formation.

Variation of Topography and Film Thickness with Blend Composition. Blending PEO4 with PMMA5 caused a gradual decrease in the film thickness to the value for pure PMMA (Table 4). The topography also changed with PMMA content, with the initially rough, angular features becoming smoother (Figure 4b−g). At PMMA contents >60% w/w the topography exhibited the rounded features observed in other studies with partially compatible amorphous blends. As the PMMA content was increased to high values, the density of features increased and the average size decreased, a behavior similar to the poly(styrene)−poly(*p*-bromostyrene) system on increasing the poly(styrene) component.[9] In the latter system though, except in the blend composition range where they became too large and overlapped, the raised features were separate, while with the PEO−PMMA blends the features are less well defined and are always more contiguous.

XPS/SIMS. The surface compositions of the blends, determined by XPS and SIMS, are shown in Figure 5. Considering first the SIMS data, the surface and bulk compositions are similar for PMMA bulk monomer fractions ≥0.3. Below 0.3 bulk fraction there is an definite excess of PMMA at the surface. The XPS data show a more complicated behavior. For PMMA bulk fractions ≥0.6 the surface and bulk compositions are the same. Below PMMA bulk fraction 0.3 there is a small excess of PMMA at the surface, but from bulk fraction 0.3−0.5 there is a marked deficit of PMMA. Disagreement between the SIMS and XPS data for a given bulk fraction indicates a concentration gradient at the surface, the former technique probing ca. 0.5−1 nm and the latter ca. 5 nm. When the techniques disagree, the SIMS data show a greater surface fraction of PMMA than the XPS. Thus, the concentration gradient is caused by a thin overlayer which is PMMA-rich.

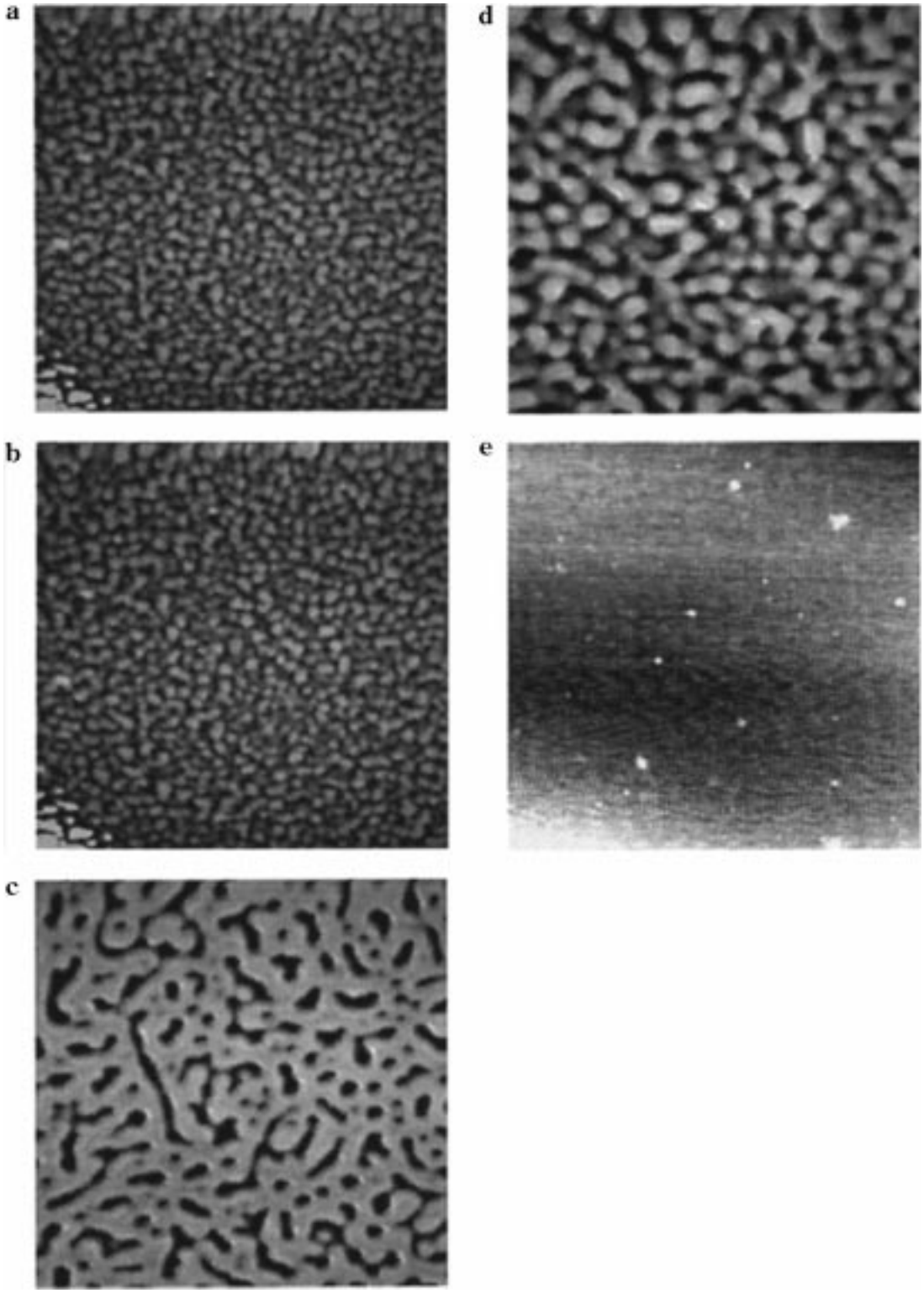

Figure 3. Topography of 75% w/w PMMA blends of various molecular weight combinations. PEO:PMMA: a, 116K:54K; b, 116K:71K; c, 116K:114K; d, 116K:320K; e, 11K:114K.

Returning to the AFM results (Figure 4), the influence of the crystalline structure of the PEO homopolymer is apparent in the images for the high PEO blends. In mixtures of amorphous and crystalline polymers there is a tendency for the amorphous material to segregate to the surface.[17] Addition of a small amount of the amorphous polymer would result in the PEO crystallites being covered by the PMMA, thereby accounting for the surface segregation observed by SIMS below 0.3 PMMA bulk fraction.

Table 3. Effect of Molecular Weight on Topography at Constant 75% w/w PMMA Blend Composition

Figure	M_n of components of blends, kg mol^{-1}	film thickness, nm	typical height/depth, nm
3a	PEO(116)/PMMA(54)	50 ± 2	49 ± 8
3	PEO(116)/PMMA(71)	73 ± 9	57 ± 11
3	PEO(116)/PMMA(114)	104 ± 14	81 ± 18
3d	PEO(116)/PMMA(320)	252 ± 9	125 ± 26
3e	PEO(11)/PMMA(114)	33 ± 6	

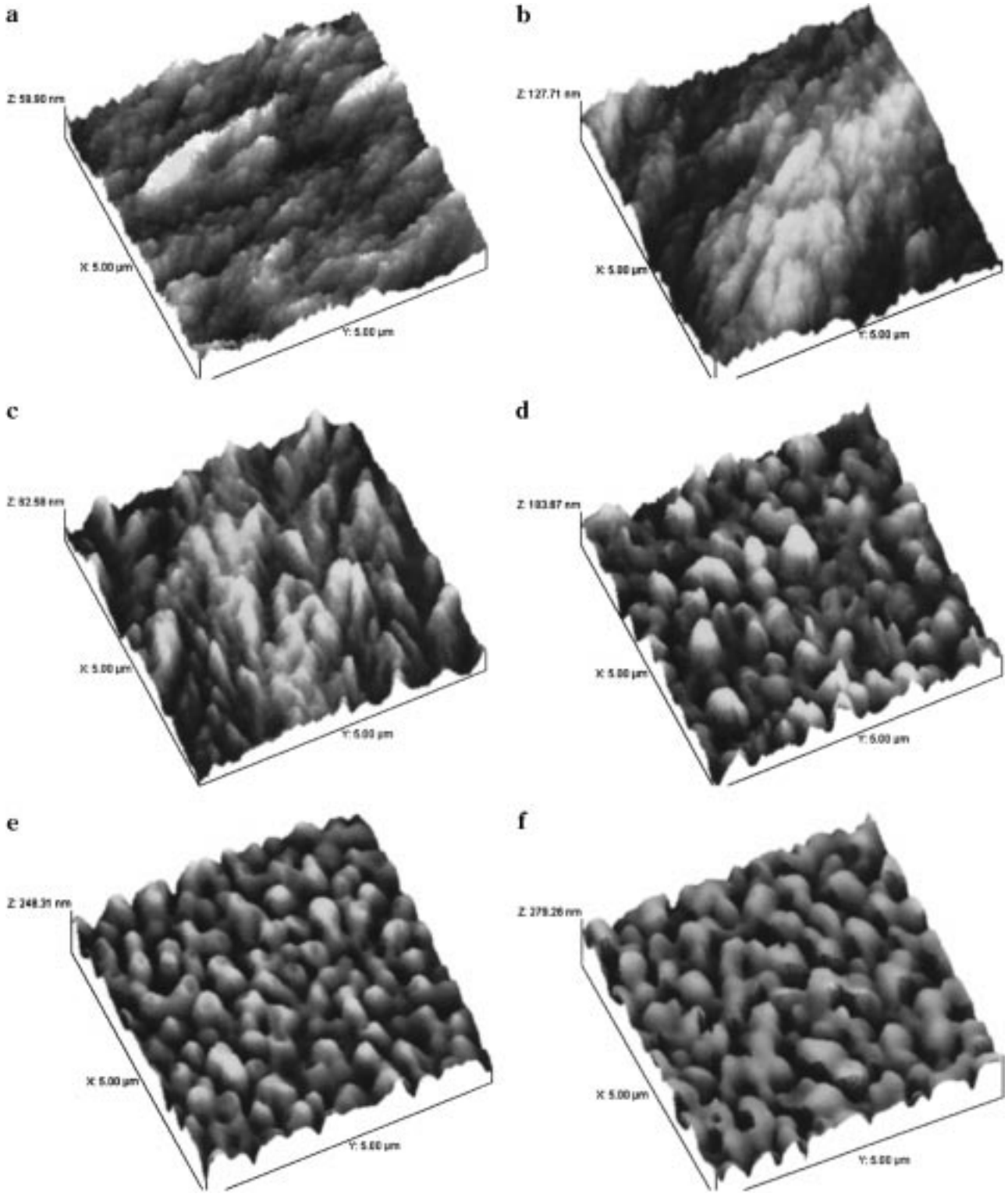

At ca. 0.3 PMMA bulk fraction there is change in the system. Between PMMA bulk fractions 0.3−0.6 (50−77% w/w) the SIMS data correspond to the bulk composition while the XPS data show a marked deficit of PMMA; i.e., the subsurface is rich in PEO. The AFM images bear less resemblance to pure PEO and show a rounding of the features. The thin, "pure" PMMA overlayer, observed for the films with fraction PMMA < 0.3, is replaced by an overlayer similar to the bulk in overall composition, while the subsurface has an excess of PEO, even though the bulk PMMA concentration is increased. Schantz showed by NMR that crystalline PEO and an amorphous PEO−PMMA phase of ca. constant composition coexist for blends with <70% w/w PMMA.[6] For annealed blends between 40 and 60% w/w PMMA, Parizel et al.[4] report a constant PMMA−PEO amorphous phase, ca. 90:10 composition, with varying amounts of partially crystalline PEO. Our XPS data, showing an excess of PEO, suggest that PEO crystallites are clustered near the surface. If the PEO phase is formed by crystallization from a PEO-rich metastable state, as postulated by Parizel et al.,[4] at the surface, then the remaining material will be richer in PMMA. The crystallites would be covered by the amorphous

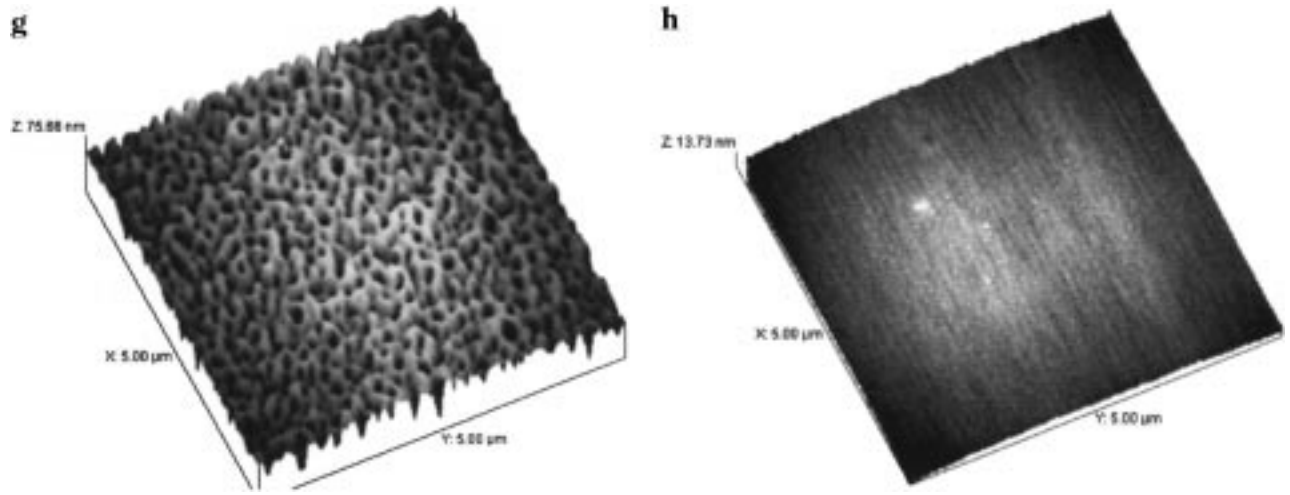

Figure 4. Topography of homopolymers and blends of various compositions, % w/w, of PMMA5 and PEO4. PEO:PMMA: a, 100:0; b, 90:10; c, 70:30; d, 50:50; e, 30:70; f, 25:75; g, 10:90; h, 0:100.

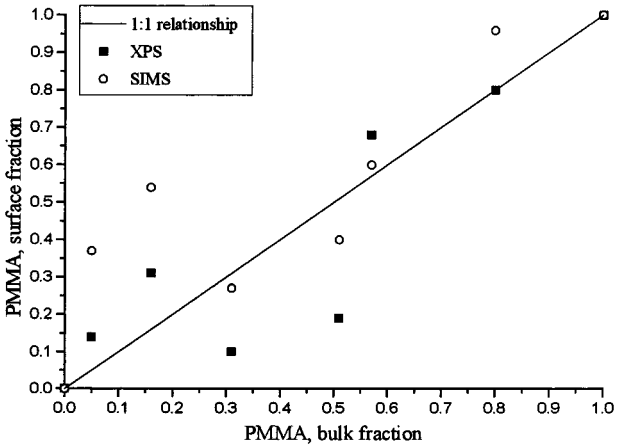

Figure 5. Surface composition, determined by XPS and SIMS, versus composition of blends of PEO4 and PMMA5.

Table 4. Variation of Topography with Composition for Blends of PEO4 and PMMA5

Figure	blend composition, % w/w PMMA	blend composition, monomer fraction PMMA	film thickness, nm
4a	0	0	621 ± 366
4b	10	0.05	675 ± 300
4c	30	0.16	523 ± 128
4d	50	0.31	366 ± 97
4e	70	0.51	253 ± 20
4f	75	0.57	246 ± 27
4g	90	0.80	187 ± 10
4h	100	1.0	173 ± 15

residue which, from the SIMS data, approximates to the bulk composition. The film does not reach an equilibrium state, which requires prolonged annealing, but is frozen at the point when evaporation of solvent has decreased the mobility of the chains to a critical level.

Above 0.6 PMMA bulk fraction (77% w/w) there is a further change in the chemical structure but little obvious change in the topography. The surface compositions from XPS and SIMS are similar and close to the bulk value; i.e., there is no concentration gradient at the surface. High PMMA blends are reported to be only entirely homogeneous, with negligible amounts of crystalline PEO, after annealing. Therefore, the distinct topography of the unannealed film surface implies a two-phase structure, and it is necessary to invoke again the concept of precursor metastable states with the role of the substrate surface being to nucleate the phases. Spin-casting the sample, which involves application of a shear stress, may also induce partial alignment of the PEO molecules, aiding crystallization.

Annealed Films. The cast films are in a nonequilibrium state because of the rapid evaporation of solvent. Annealing experiments (Figure 6) were carried at 90 and 150 °C to investigate the stability of the structures. The former temperature is above the T_g and melting point of PEO and below the T_g of PMMA. Addition of PEO to PMMA lowers the T_g of the blend to less than 90 °C for PMMA contents <90% w/w.[4] Heating a 30% w/w PMMA blend to 90 °C for 2 h caused features on the angular film to become much more diffuse, and heating to 150 °C for 30 min gave a completely smooth surface. In contrast, a 75% w/w PMMA blend retained its features after 2 h at 90 °C, but they were completely removed after heating for 1 h at 150 °C. Thus, the annealing experiments distinguish between the angular and the rounded features observed by AFM. The former were attributed to crystalline PEO. Therefore, the latter must consist mainly of PMMA.

After heating the 30% w/w PMMA blend at 150 °C to remove the topographical structures, the XPS and SIMS showed that the now smooth surface was rich in PMMA (Figure 7). At this bulk composition the annealed film will be partially crystalline. The changes in topography between the fresh and annealed films can be rationalized if the initial deposition results in assemblies of PEO crystallites and a ca. pure PMMA phase. Annealing allows the PMMA to penetrate the PEO assemblies, filling the interstices with a PEO−PMMA amorphous phase, produced by partial reaction at the crystallite surface. Because of the tendency of amorphous material in an amorphous−crystalline mixture to migrate to the surface, the PEO−PMMA phase will cover the crystallites, and both SIMS and XPS show a high PMMA content. The agreement between the SIMS and XPS, in contrast to the data for the fresh film, shows that the minimum overlayer thickness of the PEO−PMMA phase is ca. 5 nm, and the high PMMA content of the PEO−PMMA phase found by surface analysis is consistent with the reported bulk data.[4,6]

The XPS and SIMS surface compositions of the 75% w/w PMMA blend (Figure 7) were the same as the bulk value before and after heating to 150 °C for 1 h, which produced a smooth surface. The XPS/SIMS results for

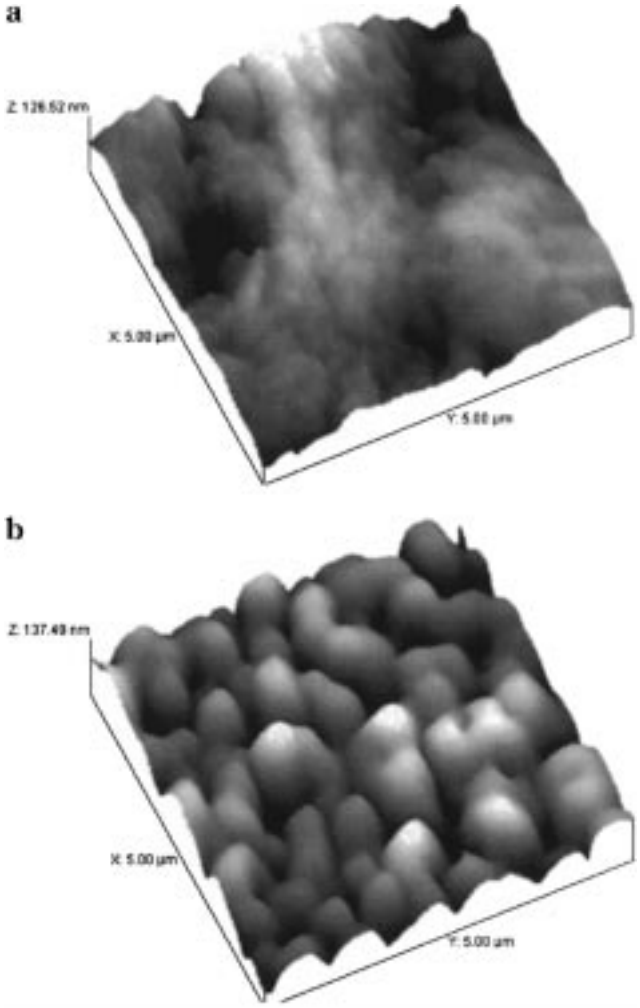

Figure 6. Topography of blends of PEO4 and PMMA5 annealed at 90 °C for 2 h: a, 30% w/w PMMA; b, 75% w/w PMMA.

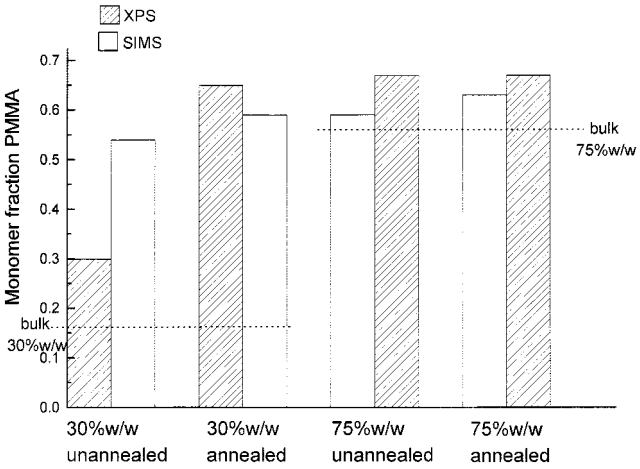

Figure 7. Surface composition, from XPS and SIMS, for 30:70 and 25:75% w/w blends of PMMA5:PEO4 before and after annealing at 150 °C.

the higher PMMA fraction films show the same trends as the XPS data of Sakellariou[18] for annealed blends of PEO and PMMA, which showed no surface segregation at high weight fractions PMMA. There is also evidence in his XPS data of segregation of PMMA in annealed low PMMA fraction blends.

An annealed 75% w/w blend is considered to be homogeneous, and for miscible polymers the component

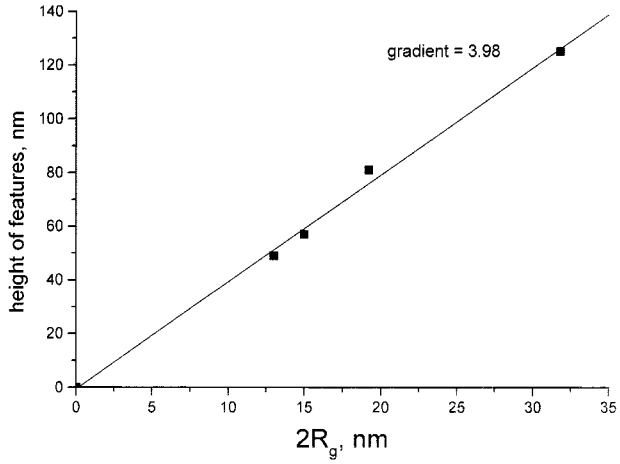

Figure 8. Relationship between AFM feature height and PMMA molecular weight.

with the lower surface tension, PMMA, may segregate to the surface depending on the relative effects of reduction of surface energy compared to loss of entropic and enthalpic contributions in the bulk. The interaction between PEO and PMMA is favorable for mixing with a small interaction parameter,[2] which is suggested by Sakellariou[18] to explain the lack of observed segregation of PMMA with an annealed homogeneous blend.

Relation between PMMA M_n and AFM Feature Height. Figure 3 and Table 3 show the AFM data for a series of blends of constant composition, 75% w/w (0.57 monomer fraction) PMMA, where the PEO M_n is constant and the PMMA M_n varies. Having established, from annealing, that the topographical features of high PMMA blends are mainly PMMA, the effect on the blends of varying M_n can be ascertained. First, a semiquantitative evaluation of the AFM data is obtained by considering the relative molar volumes, and hence the relative molar areas, of PEO and PMMA. XPS and SIMS indicated that the surface and bulk concentrations for blends of this bulk composition are similar. The area occupied by a PMMA monomer is ca. 1.7 times that of a PEO monomer. The composition of these blends is 0.57 monomer fraction PMMA, corresponding to an area fraction of 0.69. An estimate of the fraction area covered by the features was obtained for the blend with PMMA M_n 114K, by cutting an outline of the features from an AFM image and weighing, giving a value of 0.63, in agreement with the XPS and SIMS, both of which effectively "see" a 2-D view of the sample. Inspection of the images for the blends of PEO with PMMA 71K and PMMA 320K shows that the area fractions occupied by PMMA are similar.

Now, the radius of gyration of a blend component is related to the square root of M_n, and using the value of average statistical segment length for PMMA, the gyration radius can be estimated.[10] Hence, for the series of 75% w/w blends a plot of the AFM average feature height versus the gyration diameter can be obtained (Figure 8). A linear correlation is observed, with a gradient of four and an intercept close to zero, which implies that the differential in the height of the PEO and PMMA regions corresponds, on average, to aggregation of four PMMA molecules.

Considering models of the film structure, the simplest case would be a layer of PEO with an partial overlayer of PMMA, four molecules thick. The most accurate measurements will be for the thickest film, PEO 116K–

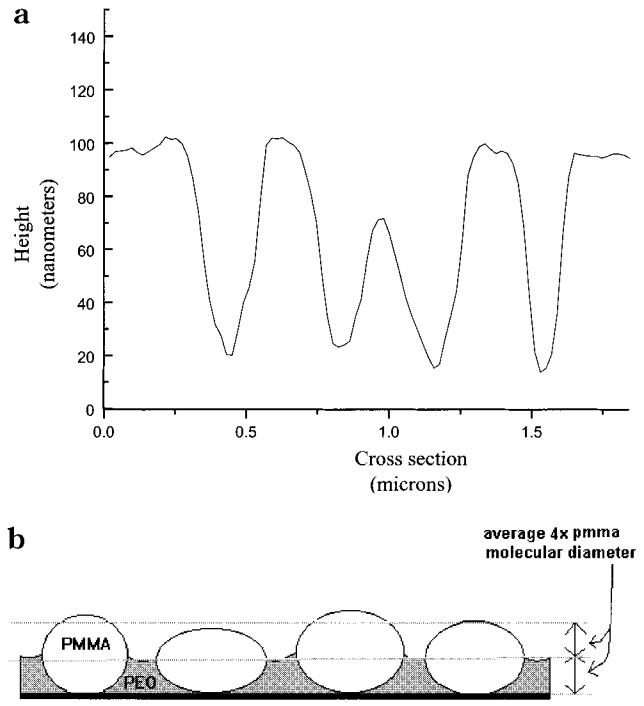

Figure 9. (a) AFM profile for PEO(116K)/PMMA(114K) blend. (b) Model of film structure.

PMMA 320K, and taking into account the feature height being 50% of the overall film thickness and the overlayer being incomplete, the relative volume of the PMMA is markedly less than that of the PEO, contrary to the bulk volume fraction, making such a model unlikely.

Another model, similar to that proposed for polystyrene−polybromostyrene,[9] is contiguous blocks of the phases anchored to the substrate surface. The total PMMA thickness would then correspond to the total film thickness, i.e., 8 PMMA molecular diameters in the case of the PEO 116K−PMMA 320K blend, because the feature height is 50% of the film thickness. An estimate of the PMMA volume fraction can be obtained from the PMMA area, the film thickness, and the step height, and taking initially a rectangular block model, as for polystyrene−polybromostyrene, would give a value of 0.88, compared to the bulk value of 0.74. Though the shape of the PMMA block adjacent to the substrate is unknown, the AFM profile shows the shape of the protruding portion (Figure 9). The features are not rectangular, in contrast to the polystyrene−polybromostyrene blends, but show a gradual increase to a peak at the center of the feature. Consequently, the volume of the PMMA is overestimated by a rectangular block model, and the true volume fraction of the PMMA will be nearer the bulk value. Thus, the structure of the film is consistent with separate phases, each made up of contiguous blocks, in contact with the substrate (Figure 9). Differences in film structure between PEO−PMMA and polystyrene−polybromostyrene may relate to the compatibility of the former and incompatiblity of the latter blend. The relationships between area fraction, observed by AFM, XPS, and SIMS, and bulk composition also differ. The AFM area fraction of PMMA is related to the monomer area fraction, whereas the polybromostyrene AFM area fraction is proportional to the monomer molar fraction.

Returning to the remainder of the blends with variable PMMA M_n, the thickness of the film and feature height both depend on the molecular weight, but the relationship between feature height and film thickness is prone to error. Although the feature height apparently approaches 100% of the film thickness at the lowest PMMA M_n and only ca. 50% of the thickness at the highest M_n, it should be noted that the feature height and overall film thickness are determined by different instruments employing different algorithms, comparisons will not be exact, and errors will be greatest for the thinnest films. Assuming that the features are PMMA, the thinnest film would contain negligible PEO if the AFM and profilometer were both accurate absolutely. The fact that the differential height relationship, $\equiv$4 molecules of PMMA, is maintained suggests that the blends are all formed similarly. It is probable that the aggregation of PMMA molecules within the films is constant, and the apparent discrepancies are caused by a systematic error. Taking the thickest film as likely to be the most accurate, a feature height of ca. 50% of the film thickness would be obtained for all the blends if there was an absolute error of ca. 5 nm between the AFM and profilometer data. Therefore, the hypothesis is proposed that the structure of all the films is as shown diagrammatically in Figure 9. The AFM profiles show that there is variation in the local film thickness, but the average step height of the PMMA blocks is $8R_g$.

Conclusion

Thin films of PEO−PMMA blends exhibit a complex behavior because of the semicrystallinity of the polyether. The progression of metastable phase structures through to smooth annealed surfaces may be followed by AFM. At low PMMA compositions the thickness of cast films is greatest, and the topography is similar to the distinctive structure of the PEO homopolymer; i.e., the crystalline PEO phase dominates the topography. Higher PMMA concentrations produce rounded topographical features which are postulated to be a mainly PMMA phase. The formation of rounded topography on unannealed films, similar to that observed with partially compatible amorphous polymer blends, suggests that, at high PMMA fractions, spin casting leads to two noncrystalline metastable phases being deposited, i.e., PEO- and PMMA-rich phases, respectively.

Annealing the films removed the topography. XPS and SIMS showed that the surface of the low PMMA annealed blends is dominated by PMMA whereas the surface of the high PMMA blends is similar in composition to the bulk.

For blends of constant PEO M_n and fixed composition but varying molecular weights of PMMA, a linear correlation is obtained between the AFM feature height and the radius of gyration of the PMMA with a gradient of $8R_g$. A model is proposed of a bicontinuous phase structure.

Acknowledgment. S. A. O'Neill is grateful to EPSRC for funding.

References and Notes

(1) Liberman, S. A.; Gomes, A. de S.; Macchi, E. M. *J. Polym. Sci., Polym. Chem.* **1984**, *22*, 2809.
(2) Cimmino, S.; Martuscelli, E.; Silvestre, C. *Polymer* **1989**, *30*, 393.
(3) Hopkinson, I.; Kiff, F. T.; Richards, R. W.; King, S. M.; Farren, T. *Polymer* **1995**, *36*, 3523.
(4) Parizel, N.; Laupretre, F.; Monnerie, L. *Polymer* **1997**, *38*, 3719.
(5) Russell, T. P.; Ito, H.; Wignall, G. D. *Macromolecules* **1988**, *21*, 1703.

(6) Schantz, S. *Macromolecules* **1997**, *30*, 1419.
(7) Straka, J.; Schmidt, P.; Dybal, J.; Schneider, B.; Spevacek, J. *Polymer* **1995**, *36*, 1147.
(8) Burdin, A. B.; Tager, A. A. *J. Polym. Sci., Part B: Polym. Phys.* **1995**, *37*, 203.
(9) Affrossman, S.; Henn, G.; O'Neill, S. A.; Pethrick, R. A.; Stamm, M. *Macromolecules* **1996**, *29*, 5010.
(10) Tanaka, K.; Takahara, A.; Kajiyama, T. *Macromolecules* **1996**, *29*, 3232.
(11) Walheim, S.; Böltau, M.; Mlynek, J.; Krausch, G.; Steiner, U. *Macromolecules* **1997**, *30*, 4995.
(12) Ermi, B. D.; Karim, A.; Douglas, J. F. *J. Polym. Sci., B: Polym. Phys.* **1998**, *36*, 191.
(13) Affrossman, S.; O'Neill, S. A.; Stamm, M. *Macromolecules*, in press.
(14) Overney, R. M.; Leta, D. P.; Fetters, L. J.; Liu, Y.; Rafailovich, M. H.; Sokolov, J. *J. Vac. Sci. Technol.* **1996**, *B14*, 1276.
(15) Overney, R. M.; Guo, L. T.; Totsuka, H.; Rafailovich, M.; Sokolov, J.; Schwarz, S. A. *Mater. Res. Soc. Symp. Proc.* **1997**, *464*, 133.
(16) Briggs, D.; Beamson, G. *Anal. Chem.* **1992**, *64*, 1729.
(17) Brant, P.; Karim, A.; Douglas, J. F.; Bates, F. S. *Macromolecules* **1996**, *29*, 5628.
(18) Sakellariou, P. *Polymer* **1993**, *34*, 16.

MA980804N